International Journal of Environmental Sciences ISSN: 2229-7359 Vol. 11 No. 24s, 2025 https://theaspd.com/index.php

# Development of Enteric-Coated Resveratrol-Loaded Eudragit S-100 Microparticles for Targeted Colonic Delivery in Colitis Management with Qbd Approach

Nikunj Agarwal<sup>1,2</sup>, Aviral Jain<sup>2</sup>, Daisy Arora<sup>3</sup>, Bharat Khurana<sup>1\*</sup>

<sup>1</sup>Adarsh Vijendra Institute of Pharmaceutical Sciences, Shobhit University, Gangoh, Uttar Pradesh, India <sup>2</sup>Gyan Sagar College of Pharmacy, Sagar, Madhya Pradesh, India

<sup>3</sup>Department of Pharmacy, Panipat Institute of Engineering and Technology, Panipat, Haryana, India Correspondence: Dr. Bharat Khurana

Adarsh Vijendra Institute of Pharmaceutical Sciences, Shobhit University, Gangoh, Uttar Pradesh, India, https://orcid.org/0000-0002-5667-2709

Email: bharatkhurana85@gmail.com

## **ABSTRACT**

This study aimed to develop and optimize resveratrol·loaded microparticles for targeted delivery in colitis using a Quality by Design (QbD) approach. Microparticles were prepared by using the emulsification-solvent evaporation method, with critical process parameters and material attributes systematically varied according to a Box-Behnken design. Among 17 formulations, the optimized batch was obtained at  $X_1$  = 5.268% tristearin concentration,  $X_2$  = 975 rpm stirring speed, and  $X_3 = 2.51\%$  PVA concentration, followed by Eudragit S-100 coating to achieve pHresponsive release. The optimized formulation demonstrated uniform spherical microparticles with desirable particle size distribution, entrapment efficiency above 85%, and reproducible drug content. Invitro release studies confirmed negligible drug release under gastric and intestinal pH, with sustained release at colonic pH, validating the suitability of the coating strategy. Entrapment efficiency was calculated indirectly by quantifying unentrapped drug in the supernatant after centrifugation and dilution in solvent, ensuring complete solubilization before analysis. Microparticles equivalent to 50 mg of resveratrol (≈ 590 mg microparticles) were used for dissolution studies to maintain dose uniformity across all formulations. Cytotoxicity studies in Caco-2 cells using the MTT assay showed that PRS, RUMP, and RCMP maintained >90% viability across 5-100 µM concentrations, with no significant trend observed (p > 0.05); minor fluctuations were attributed to normal assay variability. As per the resultfinding, the study established a robust QbD-optimized microparticle system capable of delivering resveratrol efficiently to the colon, highlighting its therapeutic potential for colitis management. The developed system presents a viable approach to resveratrol delivery that targets the colon in the management of colitis.

Keywords: Ulcerative Colitis, Resveratrol, Microparticles, Colon-Targeted Drug Delivery, Eudragit S-100, Quality by Design (QbD)

### INTRODUCTION

In terms of both treatment effectiveness and patient compliance, UC, which is a chronic inflammatory bowel disease, is difficult to manage. The colonic mucosa becomes inflamed and ulcerated in UC, resulting in symptoms like diarrhoea, abdominal pain, and rectal bleeding [1, 2]. Anti-inflammatory medications, immunosuppressants, and biologics are the usual therapeutic options for UC; however, these treatments frequently have drawbacks regarding long-term management, side effects, and efficacy[3, 4]. The investigation of alternative treatments, like resveratrol, has been spurred by the growing understanding of the part inflammation and oxidative stress play in the pathophysiology of UC [5]. The use of targeted drug delivery systems, particularly those that can direct active compounds, such as resveratrol, to the affected areas of the colon, is a novel strategy for improving treatment outcomes in UC patients. This strategy seeks to reduce systemic side effects while increasing therapeutic efficacy[6-8].

The rectum and colonic mucosa are the main areas affected by UC, a chronic, idiopathic inflammatory bowel disease (IBD)[9, 10]. Recurrent episodes of inflammation, mucosal ulceration, abdominal pain, rectal bleeding, and changed bowel habits are its hallmarks [11, 12]. The illness has a major negative influence on quality of life and frequently necessitates long-term treatment or, in extreme situations, surgery [13, 14]. UC is a complex and multifactorial condition that requires effective management due to its pathogenesis, which includes immune dysregulation, environmental factors, genetic predisposition, and gut microbiota imbalance [15, 16].

Aminosalicylates, corticosteroids, immunosuppressants, and biologics like anti-TNF agents are among the current treatment approaches for UC [17]. While these treatments can reduce inflammation and induce

International Journal of Environmental Sciences ISSN: 2229-7359

Vol. 11 No. 24s, 2025

https://theaspd.com/index.php

remission, they are often associated with systemic side effects, poor patient compliance, and limited efficacy in maintaining long-term remission[4, 18]. Moreover, non-targeted drug delivery systems result in significant drug loss before reaching the inflamed colon, reducing therapeutic outcomes and increasing the risk of off-target toxicity[19, 20].

Resveratrol (3,5,4'-trihydroxy-trans-stilbene) is a natural stilbene polyphenol mainly obtained from Polygonum cuspidatum (Japanese knotweed), grapes, peanuts, and berries. Traditionally, P. cuspidatum root has been used in Chinese and Japanese medicine for inflammatory and liver ailments. As a phytoalexin, resveratrol is produced by plants under stress and contributes to their defense. Pharmacognostic studies highlight its antioxidant, anti-inflammatory, cardioprotective, and anticancer roles. These ethnopharmacological insights support its modern application in gastrointestinal disorders such as colitis [21]. Several preclinical studies have demonstrated its efficacy in reducing oxidative stress, mucosal degradation, along with pro-inflammatory cytokines reduction in experimental colitis in vivo models[22]. However, the clinical application of this polyphenolic compound is limited due to its limited aqueous solubility, poor oral bioavailability, and rapid metabolism within the upper gastrointestinal (GI) tract, necessitating an effective delivery system for targeted colonic release[23].

Colon-targeted drug delivery approacheshave been proven to be essential for improving therapeutic efficacy in UC by ensuring that the drug remains intact through the upper GI tract and releases specifically at the site of inflammation[8, 24]. Such delivery not only maximizes local drug concentration at the affected site but also minimizes systemic absorption and related adverse effects. A targeted system can also reduce dosing frequency and enhance patient adherence in chronic disease management[25].

When it comes to colonic drug delivery, formulations based on microparticles have a number of benefits, such as consistent drug distribution, increased surface area for absorption, regulated drug release, and decreased dose dumping. Better GI transit and less variation in gastric emptying time are also made possible by these multiparticulate systems. Microparticles can shield the medication from early degradation and guarantee accurate release at colonic pH levels when paired with a pH-sensitive polymer coating [26].

A common pH-dependent polymer for enteric coatings is Eudragit S-100, which is an anionic copolymer of methyl methacrylate and methacrylic acid. It is appropriate for site-specific drug release in UC therapy because it dissolves at pH ≥7.0, which is equivalent to the distal ileum and colon[27]. Its compatibility with a range of drugs, stability, and ability to form uniform coatings make it a preferred choice for enteric protection. In this study, Eudragit S-100 was selected due to its pH-dependent solubility to ensure the resveratrol-loaded microparticlesbypass the acidic environment of the stomach and the proximal regions of the small intestine, and finally release the active compound specifically in the targeted colon region. This study presents QbD-optimized, Eudragit S-100-coated microparticles for UC, developed through a full DoE-driven design space. Unlike earlier resveratrol systems, our work integrates mechanistic anti-inflammatory validation (ROS, NF-κB, cytokines) in a DSS-stimulated Caco-2 model, thereby combining regulatory-compliant optimization with disease-relevant biological readouts

## MATERIALS AND METHODS

# Materials

All reagents and chemicals used in this research were of analytical grade and were employed as received, without undergoing any further purification, ensuring consistency and reliability in experimental outcomes. Resveratrol (≥98% purity) was sourced from Thermo Fisher Scientific. Tristearin, Polysorbate 80, Polyvinyl Alcohol (PVA), Chloroform, Sodium Hydroxide, Potassium Dihydrogen Phosphate, and Methanol were acquired from LOBA Chemie. Cell culture reagents, including Dulbecco's Modified Eagle Medium (DMEM), Fetal Bovine Serum (FBS), Penicillin, Streptomycin, Gentamicin, Amphotericin B, Lglutamine, and non-essential amino acids, were obtained from Gibco (Thermo Fisher Scientific). MTT (3-(4,5-dimethylthiazol-2-yl)-2,5-diphenyl tetrazolium bromide) and the reactive oxygen species (ROS) probe H2DCFDA (2',7'-dichlorodihydrofluorescein diacetate) were purchased from Merck. Formaldehyde (4%), Methanol (100%), and Phosphate-Buffered Saline (PBS) were procured from Merck and Himedia. The nuclear factor kappa B(NF-κB) primary antibody (Cat. No. 3033T) and Alexa Fluor 488-conjugated secondary antibody were supplied by Cell Signaling Technology. Enzyme-linked immunosorbent assay (ELISA) kits for TNF-α and IL-6 were obtained from Bio-Rad, while Dextran Sulfate Sodium (DSS) was sourced from MP Biomedicals.

International Journal of Environmental Sciences ISSN: 2229-7359 Vol. 11 No. 24s, 2025

https://theaspd.com/index.php

#### Methods

# Quality by Design Approach

The Quality by Design (QbD) framework is a modern, systematic approach to pharmaceutical development that emphasizes product and process understanding, as well as risk management, to ensure predefined quality characteristics[28]. It integrates scientific knowledge and quality risk management throughout the product lifecycle[29]. In this research study, a QbDapproach was implemented with an aim todevelop enteric-coated resveratrol-loaded microparticles intended for targeted delivery of the drug to the colonic region in UC therapy. The method made it possible to identify and regulate crucial formulation and process variables that significantly influence the quality attributes of the finished optimized product.

From defining the Quality Target Product Profile (QTPP) to identifying Critical Quality Attributes (CQAs), Critical Material Attributes (CMAs), and Critical Process Parameters (CPPs), every step of formulation development was connected by the QbD paradigm [30]. To systematically assess the impact of specific variables and their interactions on the formulation's performance, statistical tools such as the Box-Behnken Design (BBD) were used. This method guaranteed consistency, reproducibility, and regulatory compliance in product development in addition to making formulation optimisation easier [31].

## Identification of Quality Target Product Profile (QTPP)

To guarantee safety, effectiveness, along patient compliance, the QTPP acts as a strategic framework that enlists the essential quality attributes of the finalformulation[32]. To create enteric-coated microparticles loaded with resveratrol for targeted colonic drug delivery in the treatment of ulcerative colitis, the QTPP was created specifically for this study.

The QTPP's main goal was to improve the therapeutic efficacy of resveratrol while mitigating systemic adverse effects by delivering it specifically to the colon in a pH-dependent, sustained manner. Because resveratrol is sensitive to both acidic and enzymatic breakdown in the upper GI tract, a microparticle system was created to shield the medication from degradation within the stomach and small intestine, releasing the drug only at the specific targeted pH of the colon, i.e., 7.0 or higher. Table 1 lists the essential components specified in the QTPP:

**Table 1:** QTPP parameters

Key Elements	Justification
Dosage form	Oral multiparticulate system (microparticles)
Route of	Oral
administration	
Therapeutic	Management of UC via targeted colonic delivery
indication	
Drug release profile	Sustained release at colonic pH (≥7.0), with minimal release at gastric and intestinal pH
Particle size range	Optimized for colonic transit and absorption (~400–900 μm)
Encapsulation	High (≥75%) to ensure therapeutic drug loading
efficiency	
Stability	Physicochemical stability under physiological and storage conditions

## Selection of Critical Material Attributes (CMAs) and Critical Process Parameters (CPPs)

Finding CMAs and CPPs is crucial for achieving the intended level of product quality, according to the QbDmodel[33]. Three important factors were chosen for the formulation of resveratrol-loaded microparticles meant for targeted colonic delivery based on the literature review, scientific justification, and initial formulation tests. Eudragit S-100 concentration  $(X_1)$ , stirring speed  $(X_2)$ , and tristearin concentration  $(X_3)$  were among them. An enteric polymer called Eudragit S-100 is essential for achieving pH-dependent release at colonic pH  $(\geq 7.0)$ , which guarantees site-specific drug delivery. Stirring speed directly influences the emulsification process, thereby affecting the particle size distribution and overall stability of the microparticles. Tristearin, a lipid matrix former, governs the internal structure of the particles and significantly impacts drug entrapment efficiency and release behavior. These independent variables were optimized at three levels: low (-1), medium (0), and high (+1), corresponding to 2%, 4%, and 6% w/v for Eudragit S-100, 800, 1000, and 1200 rpm for stirring speed, and 1%, 2%, and 3% w/v

ISSN: 2229-7359 Vol. 11 No. 24s, 2025

https://theaspd.com/index.php

for tristearin, respectively as shown in Table 2 & 3. These parameters were subjected to systematic evaluation using a Box-Behnken Design to understand their influence on the final product quality.

Table 2: Independent and dependent variables with justification

Critical Material	Justification
Attributes and Critical	
Process Parameter	
Eudragit S-100	Controls pH-dependent release at colonic pH ≥7.0; enables targeted
concentration( $X_1$ )	drug delivery.
Stirring speed (X <sub>2</sub> )	Affects droplet stabilization, particle size, and emulsion stability during
	formation.
Tristearin(X <sub>3</sub> )	Acts as the lipid matrix; affects particle structure, drug release, and
	entrapment efficiency.

**Table 3:** Independent and dependent variables with different levels

CMAs/CPP	Levels	Levels		
	-1	0	+1	
Eudragit S-100 concentration, % w/v(X <sub>1</sub> )	2	4	6	
Stirring speed, rpm (X <sub>2</sub> )	800	1000	1200	
Tristearin, % w/v (X <sub>3</sub> )	1	2	3	

# Determination of Critical Quality Attributes (CQAs)

CQAsare the measurable physical, chemical, or biological characteristics that are required to be controlled within defined limits topreserve the final product quality and performance[34]. For the optimized resveratrol microparticle system, three CQAs were identified as most critical: particle size ( $Y_1$ ), percentage entrapment efficiency ( $Y_2$ ), and drug release at colonic pH ( $Y_3$ )as mentioned in Table 4. Particle size, ideally in the range of 400–900 µm, was selected to ensure effective colonic retention and uniform transit through the GI tract. To ensure adequate drug loading, reduce formulation loss, and support sustained therapeutic levels, an entrapment efficiency of  $\geq 75\%$  was the target. To guarantee that the formulation stays intact in intestinal and gastric conditions while releasing the drug efficiently in the colonic environment—a crucial aspect of treating ulcerative colitis—drug release behaviour at pH  $\geq 7.0$  was noted. For the assessment of the influence of particular CMAs and CPPs and to attain the intended QTPP, these CQAs were employed as response variables in the optimisation process.

Table 4: Independent and dependent variables

Table 4. Independent and dependen	it variables			
CQA	Justification			
Particle Size (400–900 μm) (Y <sub>1</sub> )	Influences colonic retention, transit, and uniformity in GI			
	delivery.			
Entrapment Efficiency ≥75%(Y <sub>2</sub> )	Ensures effective therapeutic dosing and sustained release.			
Drug Release at colonic pH	Must release drug only at colonic pH, not in gastric or intestinal			
$\geq 7.0(Y_3)$	environments.			

# Optimization of Resveratrol Microparticles Using Box-Behnken Design

The Box–Behnken Design (BBD), a response surface methodology that allows for the systematic evaluation of the effects of multiple formulation and process variables on CQAs, was used to optimise resveratrol-loaded microparticles. Three independent variables were chosen for this study because they significantly affected the performance of the microparticles: the concentration of Eudragit S-100 ( $X_1$ ), the speed at which the stirring occurred ( $X_2$ ), and the concentration of tristearin ( $X_3$ ). To examine their individual and combined effects on the three CQAs particle size ( $Y_1$ ), entrapment efficiency ( $Y_2$ ), and drug release at colonic pH  $\geq$ 7.0 ( $Y_3$ ), these variables were assessed at three coded levels (-1, 0, +1). The BBD method offered a statistical model to determine the best circumstances for producing microparticles with the targeted, sustained release in the colonic region, high encapsulation efficiency ( $\geq$ 75%), and the desired particle size (400–900 µm). This design guaranteed the final formulation's robustness and reproducibility while facilitating effective experimentation with fewer runs.

International Journal of Environmental Sciences ISSN: 2229-7359 Vol. 11 No. 24s, 2025

https://theaspd.com/index.php

# Microparticle preparation technique

Using the emulsification-solvent evaporation method, resveratrol-loaded microparticles were created by combining the CPPs and selected CMAs determined by QbD. To create the organic phase, resveratrol, the lipid matrix-former tristearin ( $X_3$ ), and Polysorbate 80 were first dissolved in chloroform. Simultaneously, the aqueous phase was prepared using distilled water containing Polyvinyl Alcohol (PVA) as a stabilizer. The organic phase was added dropwise to the aqueous phase under high-speed magnetic stirring, with the stirring speed ( $X_2$ ) maintained at predefined levels (800–1200 rpm) to control emulsion droplet size, ensuring uniform microparticle formation. The resulting oil-in-water emulsion was stirred continuously to allow evaporation of chloroform, leading to the solidification of microparticles. The obtained microparticles were filtered, followed by washing with deionized water, and dying inhot air oven at  $40 \pm 2^{\circ}$ C. The dried microparticles were then subjected to coating using a solution of Eudragit S-100 ( $X_1$ ) in isopropyl alcohol, with triethyl citrate as a plasticizer, and talc as an anti-sticking compound. Subsequently, the coating dispersion was uniformly sprayed onto the microparticles in a pan coater under optimized conditions. This method ensured the development of uniform, stable, and pH-responsive microparticles suitable for colonic delivery of resveratrol.

# Coating of Microparticles

A traditional pan coating method was used to coat the resveratrol-loaded microparticles that were optimised [35]. The coating dispersion was prepared using isopropyl alcohol as the solvent, and the filmforming polymer was Hydroxypropyl Methylcellulose (HPMC E5). First, under constant magnetic stirring to create a homogenous solution, isopropyl alcohol was gradually added to Eudragit S-100, which had previously been dispersed with Triethyl Citrate (TEC) as a plasticiser. To guarantee adequate polymer hydration, a distinct aqueous dispersion of HPMC E5 was made concurrently using purified water. To attain total homogeneity, the two dispersions were then mixed and swirled for a further fifteen minutes. Tween-80 lowers interfacial tension and improves solubilization in the organic/oil phase, reducing droplet size; PVA stabilizes droplets in the external aqueous phase via steric hindrance, preventing coalescence

Talc was incorporated into the mixture as an anti-adherent, calculated based on the total dry polymer weight, and stirred further for 10 minutes to distribute it evenly throughout the coating formulation. The final coating dispersion was applied to the drug-loaded microparticles using a spray system under optimized conditions. The microparticles were uniformly tumbled within the rotating pan while the coating solution was sprayed onto the surface, ensuring even deposition and preventing agglomeration. The coating process was carefully monitored to maintain a consistent coating level, critical for achieving uniform pH-dependent release at colonic pH ( $\geq$ 7.0). The composition of the coating material used in the study has been summarized in Table 5.

Table 5: Composition of coating material used for coating

Ingredients	Amount
HPMC	1.5%
Eudragit S-100	
Dibutyl phthalate	8%
Triethyl citrate	15%
Talc	20%
Iso propyl alcohol	150ml

#### Characterization of developed microparticles and coated microparticles Size

The size of the microparticles was assessed using an optical microscope. In this process, 50 microparticles were placed on a slide, and their particle sizes were determined using a calibrated optical micrometer.

## Entrapment efficiency%

The percentage entrapment efficiency of resveratrol-loaded microparticles was determined using an indirect method [36]. The microparticle dispersion was centrifuged at 5000 rpm for 10 minutes, and the supernatant containing unentrapped drug was collected. The supernatant was appropriately diluted with methanol:water (70:30 v/v) and sonicated in a bath sonicator (Model 40050, Sheryl Medi Equip Systems, Chennai, India) for 10–15 minutes to ensure complete solubilization. The drug content was quantified from the calibration curve, and entrapment efficiency was calculated using the equation:

ISSN: 2229-7359 Vol. 11 No. 24s, 2025

https://theaspd.com/index.php

% Entrapment = 
$$\frac{\text{Entrapped drug}}{\text{Total drug}} \times 100$$

# Drug release of microparticles

By utilising USP Type II (Paddle) apparatus at 50 rpm and temperature maintained at  $37 \pm 0.5^{\circ}$ C with 900 mL of dissolution medium (pH 7.4). Added a pre-weighed quantity of microparticles.5 mL samples have been withdrawn at specific time intervals and replaced with fresh medium. The samples were filtered using a 0.45 µm membrane filter, andthe drug concentration was measured using UV-Vis spectrophotometry at 306 nm[37].

% Drug Release = 
$$\frac{\text{Ct} \times \text{V}}{\text{D}} \times 100$$

Ct = Drug concentration at time "t", V = Volume of dissolution medium, D = Total drug content.

# Fourier Transformation Infra-Red spectroscopy (FTIR)

FTIR spectroscopy was utilized to identify and analyse the structure of the samples. FTIR spectra for drug microparticles and without drug-loadedmicroparticles were recorded employing an Agilent FTIR spectrophotometer. The potassium bromide (KBr) pellet technique was employed, wherein a small amount of the sample powder was mixed with spectroscopic-grade KBr and compressed under vacuum to form a pellet. The IR spectra were then captured by scanning across the wavenumber range of 400-4000 cm<sup>-1</sup>, using Empower software for data acquisition and analysis[38].

## Shape and surface morphology

The optimized microparticles have been analysed and surface morphology using scanning electron microscopy (SEM). By applying a dried powdered microparticle sample on two pieces of double-stick tape that were secured to an aluminium stub, the process was finished[39].

# Differential scanning calorimeter (DSC)

The drug's nature has been determined by DSC, along with thermal and polymorphic transitions involved in energy fluctuation during the formulation process[40]. Resveratrol, Eudragit S100, and formulation DSC curves were evaluated using DSC (Mettler Toledo stare DS822, Germany) in perforated aluminium-sealed pans heated at a rate of 5°C/min from 10 to 340°C while in the presence of nitrogen gas (50 mL/s).

## X-ray diffractometry

Optimized formulations of coated and uncoated microparticles were subjected to XRD examination. The diffractometer used for the measurements was a wide-angle (D8 Advance from BRUKER Germany)[41]. The measurements involved measuring the X-ray scattering angle using a copper anode fixed at 45 kV and 40 mA.

## In-vitro drug release study

In vitro drug release of plain resveratrol, uncoated microparticles (RUMP), and enteric-coated microparticles (RCMP)was performedutilizing a USP dissolution test apparatus I (Lab India DS 8000) operated at 100 rpm while maintaining the temperature at  $37 \pm 0.5$ °C. The microparticle samples, accurately weighed equivalent to 50 mg resveratrol, were placed in dissolution baskets containing 900 mL of the dissolution medium. The release profile was evaluated sequentially in simulated gastric fluid (SGF) of pH 1.2 for 2 hours, followed by simulated intestinal fluid (SIF) of pH 6.8 for 3 hours, and then in simulated colonic fluid (SCF) of pH 7.4 for the remaining 19 hours, completing a total duration of 24 hours [42].

Samples of 5 mL volume were withdrawn at different time intervals, diluted correspondingly, and their absorbance was measured at 306 nm employing UV-Vis spectrophotometer. In order to maintain the volume in the dissolving medium after every sample collection at different time intervals, the same volume of the fresh media was added.

Microparticles equivalent to 50 mg of resveratrol (corresponding to approximately 590 mg of the optimized microparticles based on 85.02% entrapment efficiency) were used for each dissolution study. The samples were dispersed in 900 mL of dissolution medium under specified pH conditions and drug release was monitored.

# In Vitro Cell Culture

Caco-2 cells were cultured in Dulbecco's Modified Eagle Medium (DMEM), obtained from Gibco, which was enriched with 10% fetal bovine serum (FBS) to support cell growth. The medium was further supplemented with essential antibiotics, including streptomycin (50  $\mu$ g/mL), penicillin (50  $\mu$ g/mL), and

International Journal of Environmental Sciences ISSN: 2229-7359

Vol. 11 No. 24s, 2025 https://theaspd.com/index.php

gentamicin (50  $\mu$ g/mL), to prevent bacterial contamination. Additionally, amphotericin B (2.5  $\mu$ g/mL) was included to inhibit fungal infections. The culture media was also included L-glutamine (1 mM) to maintain optimum cellular metabolism, along with non-essential amino acids to support optimal cell function and growth. This culturing process took place in a humidified incubator maintained at a 37°C temperature, with a constant supply of a 5% CO<sub>2</sub> environment. To prepare for the experiments, the cells were sub-cultured and then grown as a single layer (monolayer) on culture plates [43].

## Cellular Viability Evaluation

MTT assessment was utilized to evaluate the cellular viability following a standard procedure. Firstly, cells were cultured in a specialized 96-well plate. The cells were subjected to varying concentrations of PRS, RUMP, and RCMP (5, 10, 20, 40, 60, 80, and 100  $\mu$ M) for 24 hours in a humidified incubator after they had reached a particular density (roughly 70% confluency). Following this procedure, an MTT solution (5 mg/mL) was installedinto each well after the liquid containing the cells was drained. Following that, the cells were incubated again for three hours ata temperature of 37°C. Lastly, to evaluate cell viability, a microplate reader was utilised to measure a particular light intensity (optical density) at a wavelength of 570 nm[44]

## Assessment of Intracellular ROS Concentrations

It was examined how the formulation affected the DSS-induced generation of ROS in Caco2 cells. Initially, the cells were plated at a density of  $1x\ 10^5$  cells per well in 12-well plates. They were then incubated with 2% DSS for 23 hours after being exposed to 5  $\mu$ M concentrations of PRS, RUMP, and RCMP for 1 hour. To determine the total ROS levels, the cells were stained with a dye called H2DCFDA (Merck) after the media was removed from the cells. For this staining step, the cells were incubated with H2DCFDA for 30 minutes at 37°C in the dark. Lastly, a BD C6 Accuri Plus device was used to analyse the stained cells using a flow cytometry technique [45].

# NF-kB assay

 $1 \times 10^6$  cells were cultured in 6-well plates, treated for 1 hour with 5 µM concentrations of PRS, RUMP, and RCMP, and then incubated for 23 hours with 2% DSS. Following treatment, the liquid (supernatant) was extracted, and the cells were collected (pelleted) by centrifugation. The cell pellet was then resuspended in a 4% formaldehyde solution to fix the cells. The cells were carefully mixed to prevent clumping and then washed again by centrifugation with PBS buffer to remove any residual formaldehyde. Next, the cells were permeabilized to allow antibodies to enter. This was achieved by incubating them with ice-cold 100% methanol on ice for 10 minutes. The methanol was then removed by washing with PBS. The permeabilized cells were then stained with specific primary antibodies against NF-kB (all diluted 1:50; cell signalling catalogue: 3033T) for an overnight hour at 4°C. Following incubation, the cells were washed with PBS again to remove unbound primary antibodies. A secondary antibody labelled with Alexa Fluor 488 (diluted 1:100) was used to target the primary antibodies, followed by another washing step with PBS. Finally, the cells were resuspended in PBS and analysed using a flow cytometer [46].

# Enzyme-Linked Immunosorbent Assay (ELISA)

Cells (1x  $10^6$ ) were grown in 6-well plates and treated with to 5  $\mu$ M concentration of PRS, RUMP, and RCMP for 1 hour, followed by incubation with 2% DSS for 23 hours. After treatment, the cell supernatant was collected, and the level of TNF-alpha and IL-6 was evaluated by ELISA. Samples were read at 450nm using a microplate reader (iMARk<sup>TM</sup> microplate absorbance reader, Bio-Rad) following the manufacturer's instructions[47].

## Storage stability studies

The optimized coated microparticle formulation was subjected to stability testing by ICH guidelines. Resveratrol-loaded microparticles were stored under two different conditions to assess their stability over time: long-term storage at a controlled temperature of  $25 \pm 2^{\circ}$ C with relative humidity (RH) maintained at  $60 \pm 5\%$ , and accelerated storage at a higher temperature of  $40 \pm 2^{\circ}$ C with  $75 \pm 5\%$  RH. The coated microparticles were sealed in aluminium foil to protect them from moisture and light. Stability was monitored over a six-month period, during which key parameters—including percentage drug entrapment and cumulative drug release—were periodically assessed to evaluate any significant physicochemical changes in the formulation.

International Journal of Environmental Sciences ISSN: 2229-7359 Vol. 11 No. 24s, 2025 https://theaspd.com/index.php

#### **RESULTS**

## Design of Experiment (DoE)

As presented in Table 1, the defined QTPP and related characteristics for the formulation of resveratrol microparticles are outlined, focusing on an enhanced sustained-release formulation designed for colonic site drug release. The Box-Behnken design was utilized for assessing theinfluence of the chosen independent variables on the final responses simultaneously. Table 6 provides a comprehensive overview of the experimental setup, detailing the 17 runs conducted according to the Box-Behnken Design, with the corresponding observations documented.

Table 6: Design Summary

Respons e	Name	Unit	Observatio n	Analysis	Minimu m		Maximu m	Mean	S.D.	
$Y_1$	Particle Size	μm	17	Polynomia 1	470	.12	958.98	666.7	20.0	
Y <sub>2</sub>	Entrapment Efficiency	%	17	Polynomia 1	65.0	)5	86.87	77.53	1.32	
Y <sub>3</sub>	Drug Release	%	17	Polynomia 66.54		97.12	85.59	1.47		
Independ	ent Variables			Responses						
Run	X <sub>1</sub> : Eudragit S100, %	X <sub>2</sub> : Stirri ng spee d, rpm	X <sub>3</sub> : Tristearin, %	Particle (µm) (Y <sub>1</sub> )	Size		ntrapment ency (Y <sub>2</sub> )	% Release	Drug (Y <sub>3</sub> )	
1	-1	-1	0	754.23 ± 21.21 75		75.12	± 1.34	80.41 ± 1.23		
2	1	-1	0	666.43± 16.09		68.23 ± 5.85		79.38± 3.56		
3	-1	1	0	500.56± 8.45		75.98 ± 2.50		82.85 ± 4.18		
4	1	1	0	489.90± 12.	489.90± 12.60		70.65 ± 3.54		97.12 ±2.13	
5	-1	0	-1	760.12± 32.	760.12± 32.56		85.27 ± 7.26		91.37 ± 4.26	
6	1	0	-1	910.56± 23.	910.56± 23.54		65.05 ± 2.41		66.54 ± 6.34	
7	-1	0	1			77.73 ± 5.83		86.79 ± 3.86		
8	1	0	1	958.89± 17.	958.89± 17.34		86.87 ± 2.98		68.15 ± 2.62	
9	0	-1	-1	720.03± 31.	.89	78.49 ± 6.17		84.69 ± 4.73		
10	0	1	-1	470.12± 18.	.37	85.25 ± 4.60		90.37 ± 1.58		
11	0	-1	1	685.34± 8.3	685.34± 8.30		70.14 ± 2.93		85.16 ± 2.73	
12	0	1	1	500.45± 18.07		81.03 ± 8.38		91.39 ± 2.04		
13	0	0	0	680.65± 5.27		73.17 ± 3.65		84.50 ± 3.41		
14	0	0	0	672.24± 16.	672.24± 16.30		81.45 ± 5.28		96.15 ± 2.06	
15	0	0	0	620.17± 21.70		84.79 ± 7.27		91.23 ± 4.21		
16	0	0	0	610.43± 24.	40	82.16	± 8.54	93.21 ± 2.86		
17	0	0	0	580.61±25.12		83.84 ± 7.15		92.36 ± 1.21		

Results are represented as Mean ±s.d., n=3

### Response analysis

## Effect variables on the particle size $(Y_1)$

The influence of CMAs and CPPs, Eudragit S-100 concentration  $(X_1)$ , stirring speed  $(X_2)$ , and tristearin concentration  $(X_3)$  on particle size  $(Y_1)$  was evaluated using a Box-Behnken Design. The perturbation plot in Figure 1 (left) and equation 1 showed that stirring speed  $(X_2)$  has a significant inverse effect on the particle size. The results obtained showed that with an increase in stirring speed from 800 to 1200 rpm, the particle size reduces considerably due to enhanced shear forces leading to finer droplet formation during emulsification.

https://theaspd.com/index.php

On the other hand, Eudragit S-100 concentration  $(X_1)$  and tristearin concentration  $(X_3)$  both show a direct effect, where increasing their concentration leads to an increase in the particle size of the formulation. This may be attributed due to the improved viscosity and matrix volume, limiting droplet breakup and resulting in larger microparticles.

Particle Size  $(Y_1) = +632.40 + 31.13X_1 - 108.25X_2 +5.37X_3 +19.25X_1X_2 + 12.00X_1X_3 + 16.25X_2X_3 + 111.55X_1^2 - 141.70X_2^2 + 103.05X_3^2$  (1)

This trend is further supported by the 3D response surface plots as demonstratedin Figure 2 (top), where combinations of high tristearin and Eudragit concentrations at low stirring speeds result in the largest particle sizes (up to 958  $\mu$ m), while lower levels combined with higher stirring speed yield much smaller sizes (as low as 470  $\mu$ m).

According to the design summary in Table 6, the observed particle size ranged from 470  $\mu$ m to 958  $\mu$ m, with an average size of 666.71  $\mu$ m and a standard deviation of 20.04, which aligns well with the QTPP requirement for colon-targeted delivery (400–900  $\mu$ m). The polynomial model fitted the data well, enabling the prediction of optimal conditions for achieving desirable particle size distribution.

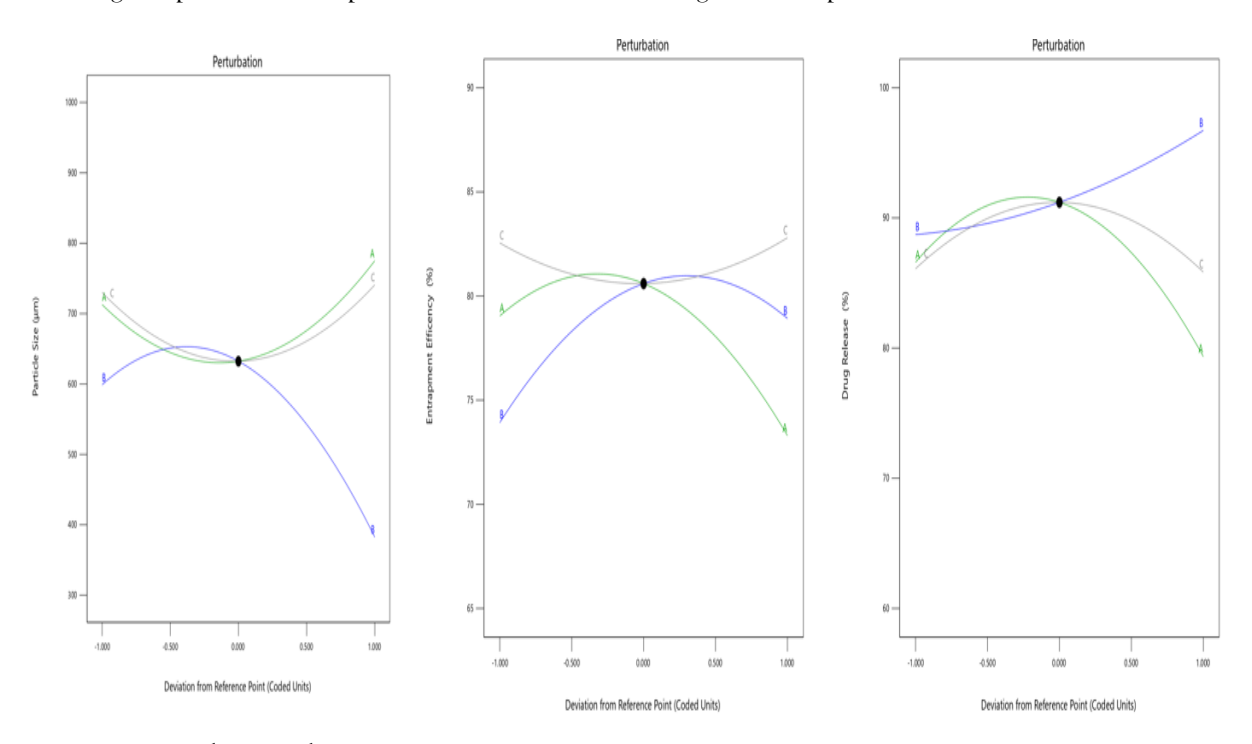


Figure 1: Perturbation plot

# Effect of Variables on the Entrapment Efficiency % % (Y<sub>2</sub>)

The percentage entrapment efficiency  $(Y_2)$  of resveratrol microparticles has been shown to have a significant influence by the selected formulation variables: Eudragit S-100 concentration  $(X_1)$ , stirring speed  $(X_2)$ , and tristearin concentration  $(X_3)$ . The perturbation plot in Figure 1 (middle) and equation 2 demonstrates that both Eudragit S-100 and tristearin had a positive impact on entrapment efficiency up to an optimum level, beyond which a slight decline was observed, indicating a quadratic relationship. Eudragit S-100 likely contributed to improved encapsulation by forming a thicker enteric coat, which reduced drug leaching during particle solidification. Similarly, an increase in tristearin concentration enhanced matrix formation, thereby entrapping more drug within the lipid phase.

In contrast, stirring speed ( $X_2$ ) exhibited a negative correlation with entrapment efficiency. Higher stirring speeds ( $\geq 1000$  rpm) generated smaller droplets with a greater surface area, increasing the likelihood of drug diffusion into the external phase, leading to reduced drug retention within the microparticles.

Entrapment Efficiency  $(Y_2) = +91.20 - 3.62X_1 + 4.00 X_2 - 0.1251X_3 + 4.0X_1X_2 + 1.75X_1X_3 + 0.001X_2X_3 - 8.23X_1^2 + 1.52X_2^2 - 5.22X_3^2$  (2)

https://theaspd.com/index.php

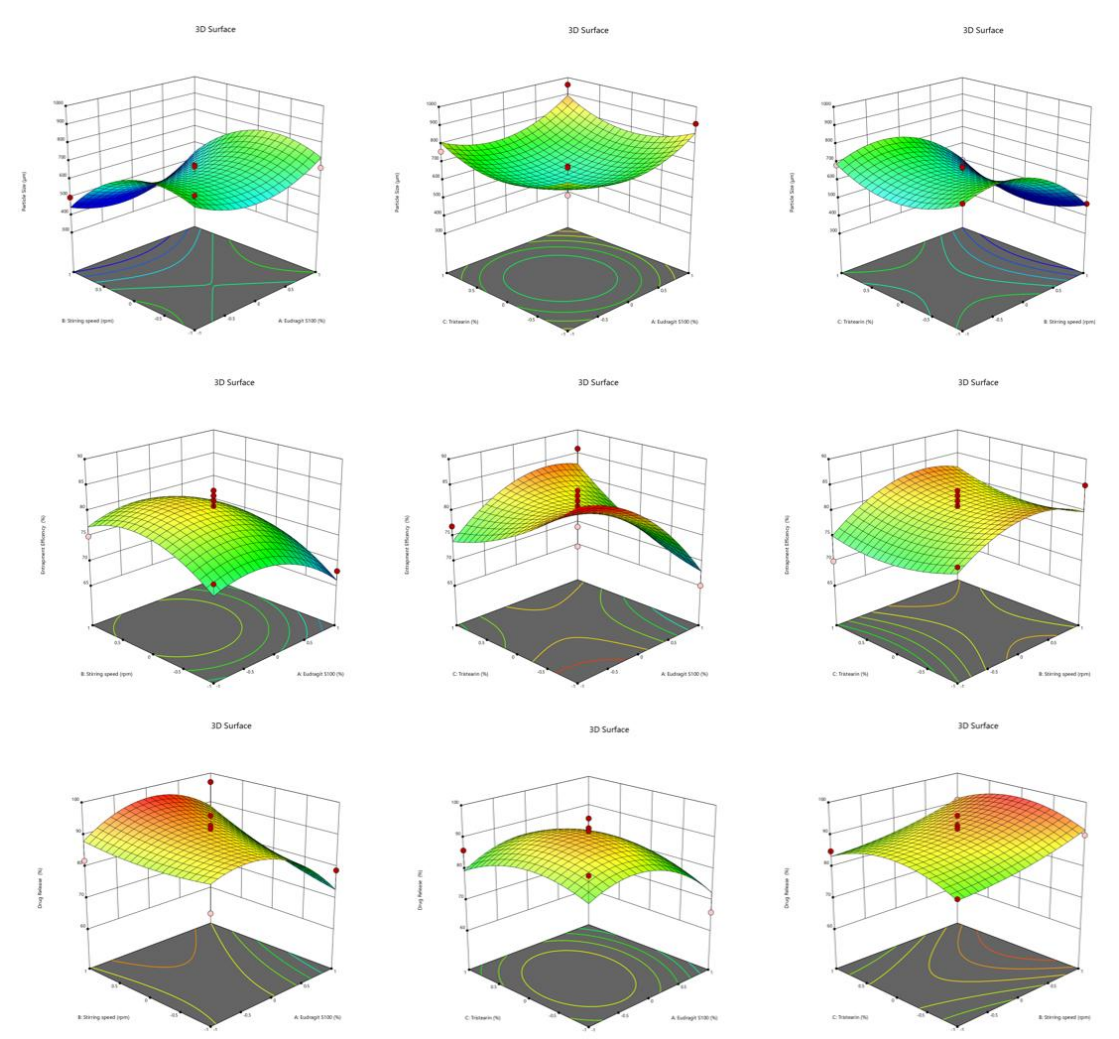


Figure 2: 3D Plots

This trend is further confirmed by the 3D surface plots in Figure 2 (middle row), where lower stirring speeds in combination with higher levels of tristearin and Eudragit resulted in maximum entrapment efficiency, reaching up to 86%, while the minimum observed value was 65%. The experimental design summary indicated a mean entrapment efficiency of 77.53% with a standard deviation of 1.32, aligning well with the QTPP requirement of ≥75%. Overall, the results validate that controlled matrix density and moderate coating levels are essential to maximize entrapment while avoiding excessive shear that can compromise drug loading.

## Effect of Variableson Drug Release (Y<sub>3</sub>)

The drug release behavior  $(Y_3)$  of resveratrol microparticles at colonic pH ( $\geq$ 7.0) was critically affected by the formulation variables: Eudragit S-100 concentration  $(X_1)$ , stirring speed  $(X_2)$ , and tristearin concentration  $(X_3)$ . The perturbation plot in Figure 1 (right)& equation 3 reveals that Eudragit S-100 and tristearin concentrations exhibited an inverse relationship with drug release. With an increase in the concentration of Eudragit S-100, the polymeric barrier became denser, delaying the drug release due to prolonged erosion or dissolution of the enteric coat at higher pH. Likewise, increased tristearin, acting as a lipid matrix, slowed down the release rate by forming a more hydrophobic core that resisted water penetration and drug diffusion.

Further, stirring speed  $(X_2)$  demonstrated a positive impact on drug release. Higher stirring speeds led to the formation of smaller microparticles with increased surface area and thinner coatings, which facilitated faster drug diffusion once the microparticles reached the colonic environment.

Drug release 
$$(Y_3) = +91.60 - 4.75X_1 + 4.88X_2 - 0.6250X_3 + 4.75X_1X_2 + 2.25X_1X_3 - 0.005X_2X_3 - 9.30X_1^2 + 1.45X_2^2 - 5.55X_3^2$$
 (3)

The 3D surface plots in Figure 2 (bottom row) illustrate those lower concentrations of tristearin and Eudragit, when combined with higher stirring speeds, resulted in maximum drug release (~97%), whereas higher polymer and lipid levels at lower stirring speeds restricted release (~66%). According to the design summary, drug release ranged between 66% to 97%, with a mean value of 85.59% and a standard

ISSN: 2229-7359 Vol. 11 No. 24s, 2025

https://theaspd.com/index.php

deviation of 1.47, fulfilling the QTPP criteria for sustained and targeted release in the colon. These findings indicate the significance of optimizing both coating and core-forming substances to balance protective properties with effective drug delivery at the desired site.

# Statistical analysis

The statistical evaluation of the experimental data was performed employing ANOVA in order to analyze the significance and predictive strength of the developed quadratic models for each response as shown on Table 7, particle size  $(Y_1)$ , entrapment efficiency  $(Y_2)$ , and drug release  $(Y_3)$ . The findings indicated that all three models were statistically significant, with p-value of 0.0103 for  $Y_1$ , 0.0001 for  $Y_2$ , and <0.0004 for  $Y_3$ , confirming that the selected formulation variables had a considerable influence on the responses.

The coefficient of determination (R²) values obtained for the evaluated parameters demonstrated a high degree of correlation between the predicted and experimental outcomes, thereby confirming the robustness and reliability of the developed model. Specifically, a R² value of 0.8954 was observed for particle size, 0.9300 for entrapment efficiency, and 0.9101 for drug release, indicating strong model fitting and minimal variability between predicted and experimental values. Furthermore, the adequate precision values, which measure the signal-to-noise ratio, were above the threshold value of 4 for Y₁ (8.363) and Y₂ (5.5746), confirming adequate model discrimination. Although the value for drug release (Y₃) was slightly lower (2.9622), it was still acceptable considering the model's overall significance.

The lack-of-fit p-values for all three responses, 0.0854 ( $Y_1$ ), 0.2703 ( $Y_2$ ), and 0.0447 ( $Y_3$ ), were greater than 0.05, demonstrating that the lack-of-fit was not significant relative to the pure error, and thus the models are suitable for prediction within the studied design space. The analysis supports the reliability of the Box-Behnken model for optimizing the formulation variables and achieving the desired critical quality attributes.

Table 7: ANOVA results

Characteristics	Particle Size (Y <sub>1</sub> )	% Entrapment Efficiency (Y <sub>2</sub> )	% Drug Release (Y <sub>3</sub> )	Remarks
Source	p-value	p-value	p-value	
Model	0.0103	0.0001	< 0.0004	Significant
R <sup>2</sup>	0.8954	0.9300	0.9101	
Mean	666.71	77.53	85.59	
Std. Dev.	68.21	5.17	8.42	
Adequate Precision	8.363	5.5746	2.9622	
Lack of Fit	0.0854	0.2703	0.0447	Not significant

## Final Optimized formulation

The desirability function analysis identified the optimal conditions at  $X_1$  = 5.268% tristearin concentration,  $X_2$  = 975 rpm stirring speed, and  $X_3$  = 2.51% PVA concentration. Under these optimized CPPs and CMAs, the final batch (Formulation 17) was prepared using the emulsification-solvent evaporation method followed by Eudragit S-100 coating. The formulation developed under these conditions yielded microparticles with desirable characteristics that closely matched the model predictions, thereby validating the robustness of the QbD approach.

# Characterization of uncoated microparticles and coated microparticles Particle Size

The optimized resveratrol-loaded microparticles exhibited a particle size of  $549.24 \pm 7.38 \, \mu m$  for uncoated and  $624.86 \pm 11.42 \, \mu m$  for coated formulations. This particle size range remains within the ideal window for colon-targeted drug delivery (400–900  $\mu m$ ), facilitating efficient colonic retention and site-specific drug release, essential for maximizing therapeutic benefit in ulcerative colitis.

# Entrapment efficiency of the drug

Entrapment efficiency (EE%) was found to be  $88.52 \pm 0.33\%$  for uncoated and  $85.02 \pm 0.91\%$  for coated microparticles. The slight drop after coating is attributed to potential surface drug loss during spray application. Slight EE% drop reflects surface drug wash-off and plasticizer-induced diffusion during spraying. The values confirm effective encapsulation, maintaining the drug within the lipid-polymeric matrix and aligning with published reports for similar delivery systems.

International Journal of Environmental Sciences ISSN: 2229-7359 Vol. 11 No. 24s, 2025 https://theaspd.com/index.php

## Drug content

Drug content was calculated as  $97.85 \pm 0.58\%$  for uncoated and  $95.74 \pm 0.75\%$  for coated microparticles, reflecting minimal loss during formulation and coating, with uniform drug distribution throughout the microparticles.

## FTIR data of Optimized Formulation

The FTIR spectra of the optimized resveratrol-loaded microparticles and the blank formulation were compared to evaluate any potential interactions between the drug and excipients as shown in figure 3a and 3b. The optimized formulation spectrum displayed characteristic absorption peaks at 3435.71 cm<sup>-1</sup> (O–H stretching), 2924.90 cm<sup>-1</sup> and 2854.06 cm<sup>-1</sup> (C–H stretching of aliphatic chains), 1638.83 cm<sup>-1</sup> (C=C aromatic stretching), 1464.62 cm<sup>-1</sup> and 1383.75 cm<sup>-1</sup> (C–H bending), and 1099.86 cm<sup>-1</sup> and 723.85 cm<sup>-1</sup> (C–O stretching and aromatic C–H bending), confirming the presence of resveratrol in its molecular form within the microparticle matrix. In contrast, the blank formulation (without resveratrol) exhibited polymer-specific peaks such as 3427.20 cm<sup>-1</sup> (O–H), 2930.08 cm<sup>-1</sup> (C–H stretching), 1632.82 cm<sup>-1</sup> (C=C and C=O stretching), and 1265.98 cm<sup>-1</sup> and 1156.38 cm<sup>-1</sup> (C–O stretching), attributed to excipients like tristearin, Eudragit S-100, and HPMC. The retention of resveratrol's functional peaks in the optimized formulation without significant shifts or new peak formation affirms that the drug and the excipients are physically and chemically compatible, and no chemical interaction occurred between the drug and the excipients during formulation. This indicates successful encapsulation and compatibility, preserving the drug's structural integrity and ensuring its therapeutic potential within the final delivery system.

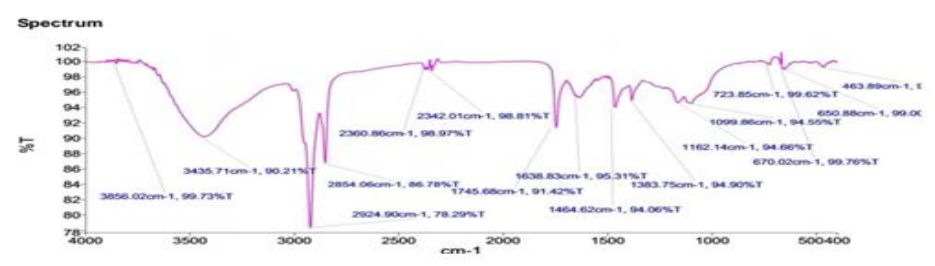


Figure 3(a): FTIR Spectra of Optimized Formulation

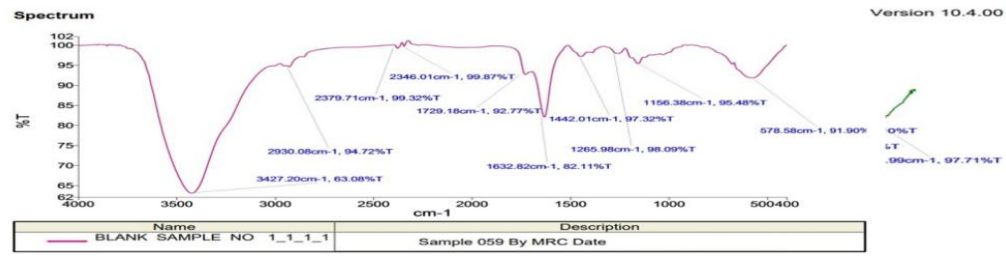


Figure 3(b): FTIR Spectra of Blank Formulation

# Morphology

The SEM image, obtained at a x30 magnification with a scale bar of  $500 \, \mu m$ , provides a detailed view of the surface morphology of the optimized resveratrol-loaded microparticles.

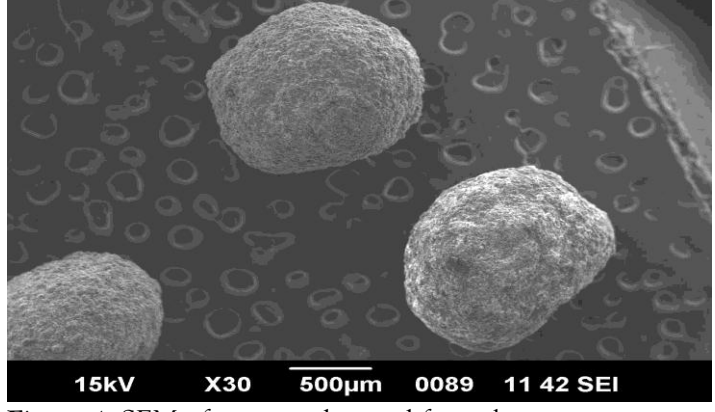


Figure 4: SEM of optimized coated formulation

The image in Figure 4 shows predominantly spherical microparticles with a rough, textured surface, indicating the successful encapsulation of resveratrol within the polymeric-lipid matrix. The uniform shape and structure of the microparticles suggest a consistent formulation process, which is crucial for achieving controlled and site-specific drug release. The visible surface characteristics, along with the particle size in the optimal range for colonic delivery, support their suitability for targeted drug delivery applications in ulcerative colitis.

# Differential scanning calorimeter

Prepared resveratrol-loaded microparticles using Eudragit S-100, as confirmed by Differential Scanning Calorimetry (DSC). The DSC thermogram in Figure 5 shows a sharp endothermic peak near 220°C, corresponding to the melting point of the drug, indicating that resveratrol was successfully encapsulated while retaining its crystalline structure. The absence of any significant shift or broadening in the peak indicates that no substantial interaction occurs between the drug and the polymer, and the formulation process preserved the thermal stability of resveratrol within the polymeric matrix.

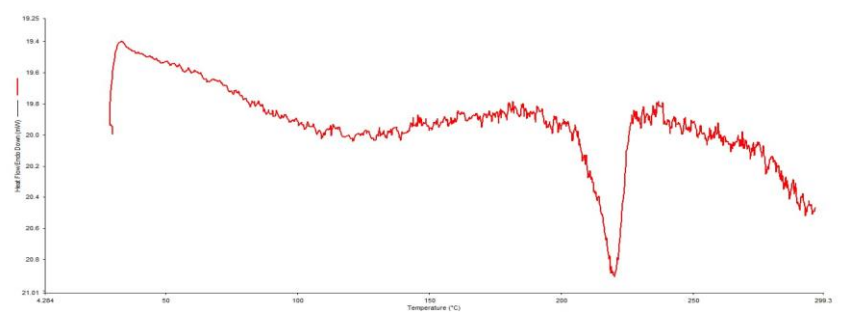


Figure 5:DSC of optimized microparticle formulation

## X-ray diffractometry (XRD)

(b)

The X-ray diffraction (XRD) patterns of the blank microparticles (Figure 6a) and resveratrol-loaded microparticles (Figure 6b) were evaluated to assess the crystalline nature and potential interaction of the drug with the polymeric matrix. The XRD pattern of blank microparticles exhibited a broad and diffused halo, indicating their amorphous nature due to the presence of polymers like Eudragit S-100 and HPMC. In contrast, the resveratrol-loaded microparticles displayed distinct but reduced intensity crystalline peaks, particularly at  $2\theta \approx 19^\circ$  and  $38^\circ$ , which are characteristic of pure resveratrol. The decrease in peak intensity and sharpness suggests that resveratrol is partially amorphized or molecularly incorporated efficiently within the polymer matrix, rather than existing in its pure crystalline form. This transformation enhances the dissolution rate and solubility of resveratrol, contributing to the sustained and colonic-targeted release profile of the microparticles.

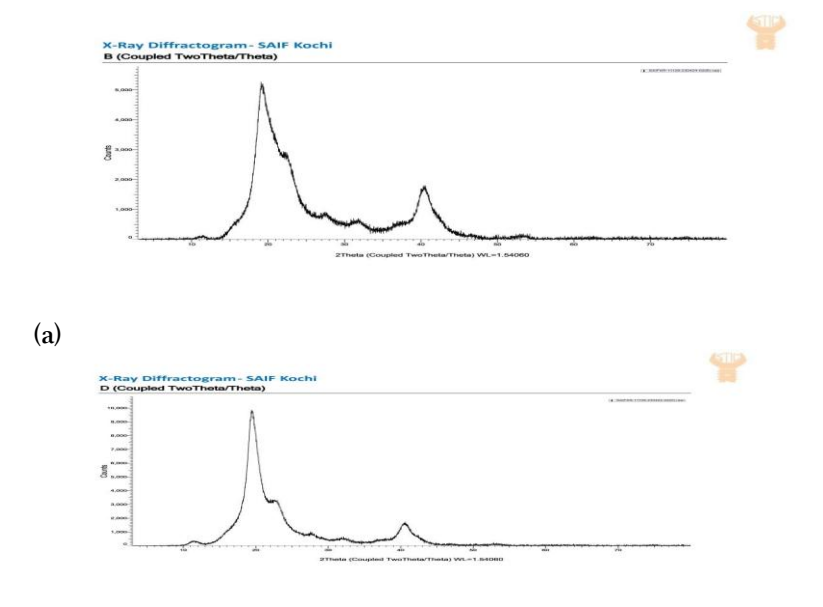
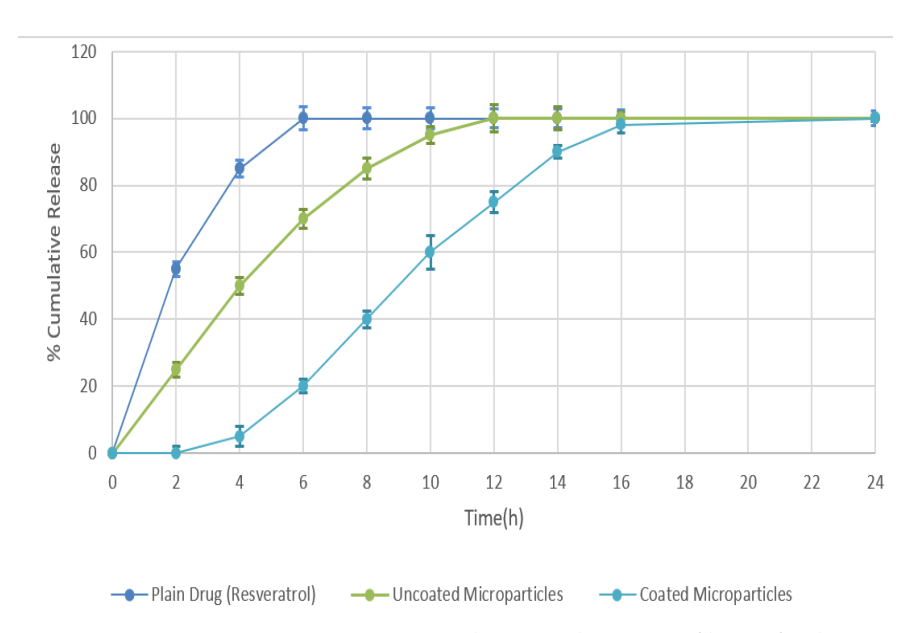


Figure. 6 (a) XRD of blank microparticles (b) XRD of resveratrol-loaded microparticles

# In-vitro drug release study

Using USP Dissolution Apparatus I (basket)approach running at 100 rpm at 37.5°C, the in vitro release profiles of plain resveratrol (PRS), uncoated microparticles (RUMP), and enteric-coated microparticles (RCMP) were assessed. The microparticles equivalent to 50 mg of resveratrol (≈ 590 mg of microparticles) were evaluated, ensuring dose uniformity and reliable comparison across formulations. Over a total duration of 24 hours, the release research was carried out in biorelevant fluids modelling GI transit: SGF (pH 1.2) for 2 hours, SIF (pH 6.8) for 3 hours, and SCF (pH 7.4) for the remaining 19 hours. Regular intervals saw the recording of cumulative drug release (%) as shown in **Figure 7**.

With almost 60% of the medication released in 2 hours and over 95% by 6 hours, the PRS formulation showed fast and prompt release, suggesting early breakdown across the stomach and intestinal stages show premature release. Extensive first-pass metabolism results from this uncontrolled release, therefore reducing the therapeutic effectiveness of resveratrol in colonic diseases. RUMP demonstrated a biphasic type of release pattern. Following an initial lag phase in the beginning in acidic medium, a gradual release during the intestinal phase produced around 90% cumulative drug release by 12 h. The lipidic matrix formulation offered some protection, yet, lacking a pH-responsive barrier hampered site-specific colonic distribution.



**Figure7:**Comparative in vitro cumulative release profiles of plain resveratrol (PRS), uncoated microparticles (RUMP), and enteric-coated microparticles (RCMP) over 24 hours in sequential simulated GI fluids: SGF (pH 1.2, 2 hours), SIF (pH 6.8, 3 hours), and SCF (pH 7.4, up to 24 hours).

The RCMP formulation, on the other hand, showed a well-regulated, pH-dependent release pattern. During the SGF and SIF phases, drug release stayed low (5–10%), verifying the acid resistance and functional integrity of the enteric coating. Exposure to SCF (pH 7.0) produced a prolonged and colonic-specific release; within 16-18 h, almost 100% drug release was attained. The efficacy of the chronotherapeutic system is emphasised by the delayed release start followed by a regulated diffusion phase, as shown in Figure 8.

The dual mechanism of medication protection explains RCMP's improved performance: Eudragit S-100 was the matrix-forming polymer for internal microparticle structuring, while hydroxypropyl methylcellulose (HPMC) was the enteric coating polymer. This architecture guarantees directed delivery to the inflamed colonic area and effectively stops early medication release in the upper GI tract.

## Cell Viability Assay

The cytotoxic effects of PRS, RUMP, and RCMP formulations on Caco2 cell lines were evaluated using the MTT assay. MTT reagent was added after Caco2 cells were incubated with different concentrations of each formulation for a predetermined amount of time in order to assess cell viability based on mitochondrial metabolic activity. The amount of formazan product produced by viable cells was assessed by determining the absorbance at 570 nm. As seen in Figure 8, cell viability stayed above 90% at all tested concentrations, indicating that PRS, RUMP, and RCMP had no discernible cytotoxic effects on Caco2

cells. This implies that, in the experimental setting, the tested formulations are safe and biocompatible with intestinal epithelial cells.

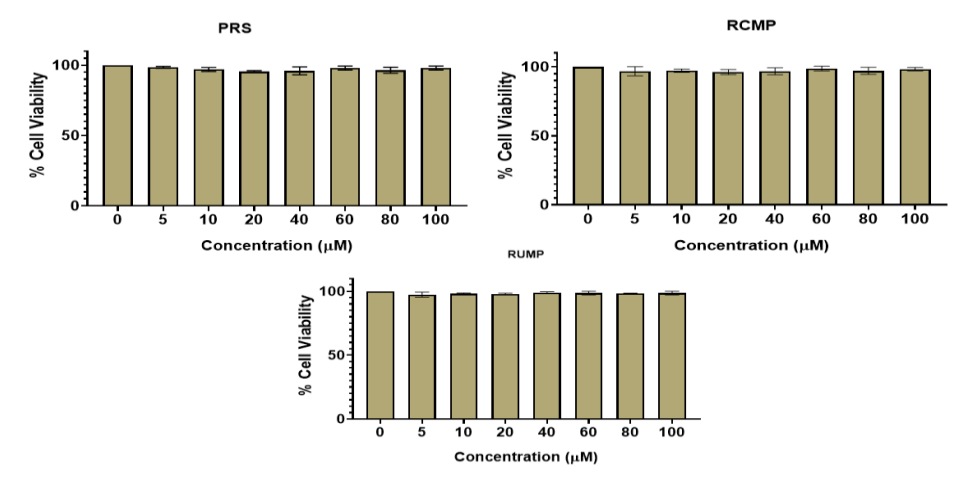


**Figure 8:**Cytotoxicity assessment of PRS, RUMP, and RCMP on Caco-2 cells using the MTT assay. Cells were exposed to varying concentrations  $(5-100\,\mu\text{M})$  for 24 h, and viability was expressed as % of untreated control (mean  $\pm$  SD, n = 3). All formulations maintained >90% viability with no significant trend observed (p > 0.05); minor fluctuations likely reflect normal assay variability at higher polymer/lipid concentrations.

## Intracellular ROS Assay

After Caco2 cells were treated with 2% DSS after being pretreated with the formulations PRS, RUMP, and RCMP, a notable decrease in the generation of reactive oxygen species (ROS) was seen (Figure 9). The pretreated groups showed significantly lower fluorescence intensity, indicating lower levels of oxidative stress, than cells exposed to DSS alone. The findings clearly indicate that all three formulations have protective antioxidant activity and can effectively reduce the production of ROS in intestinal epithelial cells caused by 2% DSS. These findings demonstrate how PRS, RUMP, and RCMP may help maintain cellular redox balance in inflammatory environments.

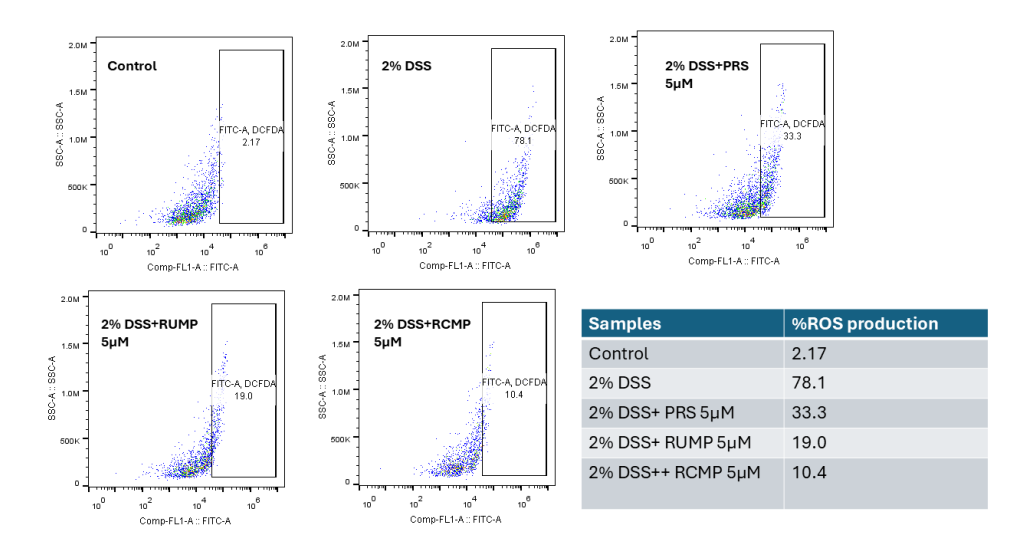


Figure9:Impact of RCMP, RUMP, and PRS on the generation of ROS in Caco2 cells caused by DSS. After an hour of pretreatment with PRS, RUMP, and RCMP (5  $\mu$ M), cells were stimulated for 23 hours with 2% DSS. Using a fluorescent probe, intracellular ROS levels were determined and expressed as fluorescence intensity. While pretreatment with PRS, RUMP, and RCMP significantly decreased ROS levels, DSS treatment significantly increased ROS production. The formulation with the highest antioxidant activity was RCMP. The data are shown as mean  $\pm$  SD (n = 3). p < 0.001 in comparison to the DSS-treated group.

https://theaspd.com/index.php

## Flow Cytometric Analysis of NF-KB Activation

Using flow cytometry, the expression of NF-kB in Caco2 cells was examined in order to learn more about the formulations' anti-inflammatory properties. After an hour of pretreatment with PRS, RUMP, and RCMP, cells were stimulated for 23 hours with 2% dextran sulphate sodium (DSS). Intracellular NF-kB levels were significantly elevated after DSS treatment, indicating the upregulation of inflammatory signalling pathways. However, the expression of NF-kB was significantly lower in cells pretreated with PRS, RUMP, and RCMP, suggesting that DSS-induced NF-kB activation was suppressed. As illustrated in Figure 10, RCMP demonstrated the most significant downregulation of NF-kB expression among the three, indicating greater effectiveness in reducing the pro-inflammatory response at the molecular level.

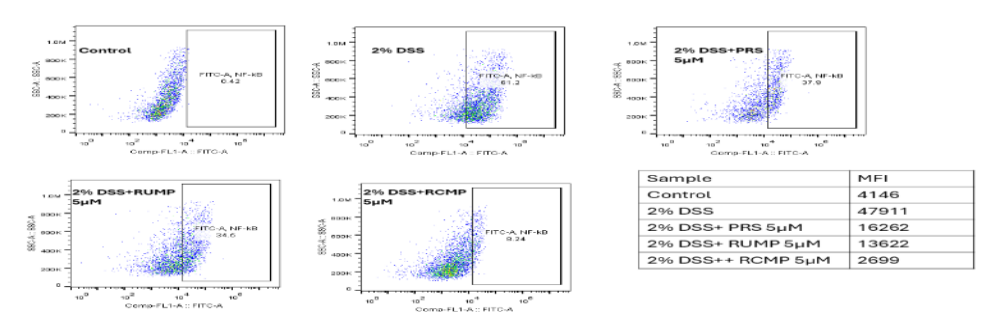


Figure 10.Effects of PRS, RUMP, and RCMP on DSS-induced NF- $\kappa$ B activation in Caco2 cells as determined by flow cytometry. After being exposed to 2% DSS for 23 hours, Caco2 cells were pretreated with PRS, RUMP, and RCMP (5 μM) for 1 hour. Utilising a particular fluorescently labelled antibody, intracellular NF- $\kappa$ B levels were found and examined using flow cytometry. The induction of the inflammatory signalling pathways was demonstrated by the significant increase in NF- $\kappa$ B expression that followed DSS treatment. Pretreatment with RCMP, RUMP, and PRS all markedly decreased NF- $\kappa$ B activation, with RCMP having the strongest inhibitory effect. The data is represented as mean fluorescence intensity (MFI)  $\pm$  standard deviation (n = 3). p < 0.01, in comparison to the group treated with DSS.

# Enzyme-Linked Immunosorbent Assay (ELISA)

To assess the anti-inflammatory potential of the optimized formulations, the concentrations of proinflammatory cytokines IL-6 and TNF- $\alpha$  were measured using ELISA as shown in Figure 11. Caco2 cells were pretreated with PRS, RUMP, and RCMP for 1 hour, followed by stimulation with 2% dextran sulfate sodium (DSS) for 23 hours to induce an inflammatory response. As expected, exposure to 2% DSS significantly elevated the extracellular secretion of TNF- $\alpha$  and IL-6, confirming inflammation. However, pretreatment with PRS, RUMP, and RCMP effectively suppressed the DSS-induced expression of both cytokines. Among the tested formulations, RCMP demonstrated the most pronounced inhibitory effect on the levels of IL-6 and TNF- $\alpha$ , demonstrating a stronger anti-inflammatory activity compared to PRS and RUMP.

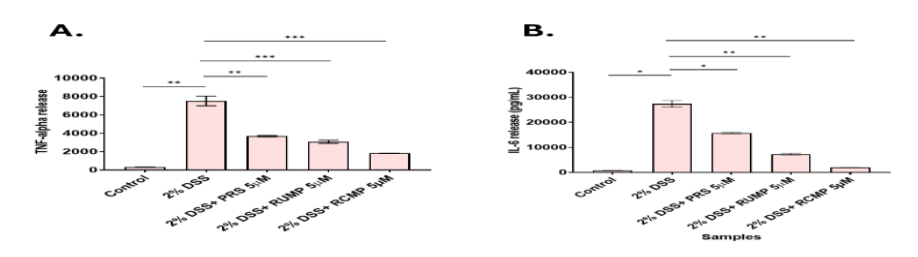


Figure 11: Effect of PRS, RUMP, and RCMP on DSS-induced secretion of IL-6 and TNF- $\alpha$  in Caco2 cells assessed by ELISA. Caco2 cells were pretreated with PRS, RUMP, and RCMP (5 μM) for 1 hour and then stimulated with 2% DSS for 23 hours. Culture supernatants were collected and analyzed for the proinflammatory cytokines levels (A) TNF- $\alpha$  and (B) IL-6 using ELISA. The treatment with DSS significantly increased the secretion of both cytokines, whereas pretreatment with PRS, RUMP, and RCMP results in a significant decrease in the levels of both cytokines. RCMP exhibited the most potent inhibitory effect on cytokine release. Data are represented as mean  $\pm$  SD (n = 3). p< 0.01 vs. DSS-treated group.

International Journal of Environmental Sciences ISSN: 2229-7359

Vol. 11 No. 24s, 2025

https://theaspd.com/index.php

Over six months, the samples were subjected to both long-term storage conditions, as recommended by the ICH guidelines, which involved maintaining a temperature of  $25 \pm 2$  °C and a RH of  $60 \pm 5\%$ , as well as accelerated storage conditions, where the temperature was set at  $40 \pm 2$  °C and RH was maintained at  $75 \pm 5\%$ , to evaluate the physicochemical stability of the optimised HPMC-coated, resveratrol-loaded microparticles (formulated using Eudragit S-100 as the matrix-forming polymer). As per the ICH Q1A(R2) recommendations, samples were extracted at specified intervals0, 60, 120, and 180 daysand evaluated for two important quality criteria (CQAs): percentage drug entrapment efficiency (%EE) and cumulative percentage drug release (%CDR).

These results validate the thermal durability and long-term chemical stability of the HPMC-coated resveratrol microparticles. Slow polymer relaxation or small surface-level drug diffusion, processes often seen in coated microparticle systems, cause the tiny declines in %EE and %CDR. Visual inspection throughout the trial showed no agglomeration, discolouration, or morphological changes, hence confirming the stability of the formulation as shown in Table 7.

**Table 7:**Stability profile of coated resveratrol microparticles showing % drug entrapment and % cumulative release over 180 days under ICH conditions.

Parameters	Stability at 25±2 °C				Stability at 40±2 °C			
Coated	0th	60th day	120th	180th	0th day	60th day 120th 180th		
Microparticl e	day		day	day			day	day
% drug entrapment	85.0 2 ± 0 .91	84.45±0 .17	84.93±0 .85	82.36±0 .53	85.02 ± 0.91	83.47±0 .83	82.26±0 .58	81.53±0 .83
% cumulative drug release	97.2 7±6. 1	95.84 56±4.9	95.39±4. 4	93.57±4. 8	97.27±6. 1	94.46±5.	93.65±3. 9	92.48±5. 8

### DISCUSSION

The experimental design optimized three key formulation variables: Eudragit S-100 concentration ( $X_1$ ), stirring speed ( $X_2$ ), and tristearin concentration ( $X_3$ ), influencing particle size ( $Y_1$ ), entrapment efficiency ( $Y_2$ ), and drug release ( $Y_3$ ). Particle size ranged from 470–958  $\mu$ m, with increased Eudragit and tristearin leading to larger particles due to higher viscosity. In contrast, faster stirring produced smaller particles due to shear-induced droplet breakup. Entrapment efficiency (65% to 86%) increased with moderate levels of Eudragit and tristearin, likely due to enhanced matrix density. However, high stirring speeds led to reduced drug retention. Drug release (66% to 97%) inversely correlated with Eudragit and tristearin levels but positively with stirring speed, which promoted faster erosion and diffusion. ANOVA confirmed statistical significance (p < 0.05) for all responses.

Optimized microparticles displayed a size of  $549.24\pm7.38~\mu m$  (uncoated) and  $624.86\pm11.42~\mu m$  (coated). Entrapment efficiency was  $88.52\pm0.33\%$  and  $85.02\pm0.91\%$  respectively. Drug content exceeded 95% in both forms. FTIR confirmed chemical compatibility, showing no interaction between resveratrol and excipients. SEM analysis revealed spherical particles with rough surfaces. DSC thermograms confirmed resveratrol stability post-encapsulation, and XRD showed partial amorphization, supporting sustained release.

Plain resveratrol (PRS) released >95% of drug within 6 h, suggesting premature upper GI release. Uncoated microparticles (RUMP) showed sustained release, achieving ~90% at 12 h. Enteric-coated microparticles (RCMP) released <10% in acidic and intestinal pH but ~100% at pH 7.4 after 16–18 h, confirming colonic targeting. The dual-layer system with Eudragit and HPMC enabled controlled delivery to inflamed colon.

MTT assays confirmed biocompatibility; all formulations maintained >90% cell viability across concentrations. DSS-induced ROS production was significantly reduced by PRS, RUMP, and RCMP, with RCMP exhibiting the strongest antioxidant response. Flow cytometry revealed suppression of NF-KB expression in treated cells, again with RCMP showing maximal effect.

ELISA results showed that DSS significantly elevated TNF- $\alpha$  and IL-6 levels in Caco2 cells. Pretreatment with PRS, RUMP, and RCMP lowered these levels significantly, with RCMP showing the highest reduction, supporting its superior anti-inflammatory efficacy.

ISSN: 2229-7359 Vol. 11 No. 24s, 2025

https://theaspd.com/index.php

Under ICH conditions, RCMP retained its integrity with minor, non-significant reductions in drug content and release over 6 months. Both long-term and accelerated storage confirmed the thermal and chemical stability of the formulation.

The optimized resveratrol-loaded microparticles, particularly the enteric-coated RCMP formulation, demonstrated targeted colonic delivery, high entrapment efficiency, prolonged release, and strong anti-inflammatory and antioxidant effects. These findings support their potential as an advanced therapy for ulcerative colitis.

## **CONCLUSION**

The present study successfully developed and optimized enteric-coated resveratrol-loaded microparticles using a QbD-based approach for colon-targeted therapy in ulcerative colitis. The Eudragit S-100 coating enabled pH-dependent drug release, effectively protecting the active compound from premature degradation and ensuring delivery at the site of inflammation. The optimized formulation demonstrated robust physicochemical characteristics, excellent in vitro release behavior, high biocompatibility, and potent anti-inflammatory activity. Stability studies further confirmed its suitability for long-term storage. Collectively, this multiparticulated livery system presents a promising strategy for enhancing resveratrol's therapeutic potential in colitis management.

**Funding:** No specific grant from a public, private, or nonprofit funding organisation was obtained for this study.

## Conflicts of interest.

The writers disclose no competing interests. The paper's writing and content are solely the authors' responsibility.

#### REFERENCES

- 1. Singh A, Kaur K, Kaur V, Singh G, Mandal UK, Mishra N, et al. Importance of nanocarriers and probiotics in the treatment of ulcerative colitis. J Drug Deliv Ther. 2019;9:216-28.
- 2. Singh A. Development Characterization and Evaluation of Mesalamine Loaded Probiotic Based Microcarriers for the Management of Ulcerative Colitis: MRSPTU, Bathinda; 2023.
- 3. Cai Z, Wang S, Li J. Treatment of inflammatory bowel disease: a comprehensive review. Frontiers in medicine. 2021;8:765474.
- 4. Ferretti F, Cannatelli R, Monico MC, Maconi G, Ardizzone S. An update on current pharmacotherapeutic options for the treatment of ulcerative colitis. Journal of Clinical Medicine. 2022;11(9):2302.
- 5. Talebi M, Talebi M, Farkhondeh T, Samarghandian S. Therapeutic effects of resveratrol in inflammatory bowel diseases: shedding light on the role of cellular and molecular pathways. Revista Brasileira de Farmacognosia. 2022;32(2):160-73.
- 6. Hani U, Honnavalli YK, Begum MY, Yasmin S, Osmani RAM, Ansari MY. Colorectal cancer: A comprehensive review based on the novel drug delivery systems approach and its management. Journal of drug delivery science and technology. 2021;63:102532.
- 7. Gowd V, Jori C, Chaudhary AA, Rudayni HA, Rashid S, Khan R. Resveratrol and resveratrol nano-delivery systems in the treatment of inflammatory bowel disease. The Journal of nutritional biochemistry. 2022;109:109101.
- 8. Lee SH, Bajracharya R, Min JY, Han J-W, Park BJ, Han H-K. Strategic approaches for colon targeted drug delivery: an overview of recent advancements. Pharmaceutics. 2020;12(1):68.
- 9. Tatiya-Aphiradee N, Chatuphonprasert W, Jarukamjorn K. Immune response and inflammatory pathway of ulcerative colitis. Journal of basic and clinical physiology and pharmacology. 2019;30(1):1-10.
- 10. Pei Ly, Ke Y-s, Zhao H-h, Wang L, Jia C, Liu W-z, et al. Role of colonic microbiota in the pathogenesis of ulcerative colitis. BMC gastroenterology. 2019;19:1-11.
- 11. Alvarez-Payares JC, Ramírez-Urrea S, Correa-Parra L, Salazar-Uribe D, Velásquez-López M, Ramírez-Urrea SI. Mucocutaneous manifestations of inflammatory bowel disease. Cureus. 2021;13(8).
- 12. Gecse KB, Vermeire S. Differential diagnosis of inflammatory bowel disease: imitations and complications. The lancet Gastroenterology & hepatology. 2018;3(9):644-53.
- 13. Olbrich KJ, Müller D, Schumacher S, Beck E, Meszaros K, Koerber F. Systematic review of invasive meningococcal disease: sequelae and quality of life impact on patients and their caregivers. Infectious diseases and therapy. 2018;7:421-38.
- 14. Armuzzi A, Liguori G. Quality of life in patients with moderate to severe ulcerative colitis and the impact of treatment: a narrative review. Digestive and Liver Disease. 2021;53(7):803-8.
- 15. Kaur A, Goggolidou P. Ulcerative colitis: understanding its cellular pathology could provide insights into novel therapies. Journal of inflammation. 2020;17:1-8.
- 16. Guo XY, Liu XJ, Hao JY. Gut microbiota in ulcerative colitis: insights on pathogenesis and treatment. Journal of digestive diseases. 2020;21(3):147-59.
- 17. Tripathi K, Feuerstein JD. New developments in ulcerative colitis: latest evidence on management, treatment, and maintenance. Drugs in context. 2019;8:212572.
- 18. Siddiqui MT, Kasiraj R, Naseer M. Medical Management of Ulcerative Colitis and Crohn's Disease—Strategies for Inducing and Maintaining Remission. Surgical Clinics. 2025;105(2):435-54.
- 19. Chen M, Lan H, Jin K, Chen Y. Responsive nanosystems for targeted therapy of ulcerative colitis: Current practices and future perspectives. Drug Delivery. 2023;30(1):2219427.

ISSN: 2229-7359 Vol. 11 No. 24s, 2025

https://theaspd.com/index.php

- 20. Fang X, Feng J, Zhu X, Feng D, Zheng L. Plant-derived vesicle-like nanoparticles: A new tool for inflammatory bowel disease and colitis-associated cancer treatment. Molecular Therapy. 2024;32(4):890-909.
- 21. Kaur A, Tiwari R, Tiwari G, Ramachandran V. Resveratrol: A vital therapeutic agent with multiple health benefits. Drug research. 2022;72(01):5-17.
- 22. Nunes S, Danesi F, Del Rio D, Silva P. Resveratrol and inflammatory bowel disease: The evidence so far. Nutrition research reviews. 2018;31(1):85-97.
- 23. Chimento A, De Amicis F, Sirianni R, Sinicropi MS, Puoci F, Casaburi I, et al. Progress to improve oral bioavailability and beneficial effects of resveratrol. International journal of molecular sciences. 2019;20(6):1381.
- 24. Saxena S, Singh C, Yadav M, Samson AL. A review on novel approaches for colon targeted drug delivery systems. PharmaTutor. 2018;6(7):11-22.
- 25. D'Amico F, Fasulo E, Jairath V, Paridaens K, Peyrin-Biroulet L, Danese S. Management and treatment optimization of patients with mild to moderate ulcerative colitis. Expert Review of Clinical Immunology. 2024;20(3):277-90.
- 26. Niazi TTK, Shah SU, Shaukat I, Rashid SA, Ullah H, Shahwani NA, et al. Journal of Population Therapeutics & Clinical Pharmacology.
- 27. Nikam A, Sahoo PR, Musale S, Pagar RR, Paiva-Santos AC, Giram PS. A systematic overview of Eudragit® based copolymer for smart healthcare. Pharmaceutics. 2023;15(2):587.
- 28. Mishra V, Thakur S, Patil A, Shukla A. Quality by design (QbD) approaches in current pharmaceutical set-up. Expert opinion on drug delivery. 2018;15(8):737-58.
- 29. Beg S, Hasnain MS, Rahman M, Swain S. Introduction to quality by design (QbD): fundamentals, principles, and applications. Pharmaceutical quality by design: Elsevier; 2019. p. 1-17.
- 30. Namjoshi S, Dabbaghi M, Roberts MS, Grice JE, Mohammed Y. Quality by design: Development of the quality target product profile (QTPP) for semisolid topical products. Pharmaceutics. 2020;12(3):287.
- 31. Szpisják-Gulyás N, Al-Tayawi AN, Horváth ZH, László Z, Kertész S, Hodúr C. Methods for experimental design, central composite design and the Box–Behnken design, to optimise operational parameters: A review. Acta Alimentaria. 2023;52(4):521-37
- 32. Furlanetto S, Orlandini S, Pieraccini G, Gotti R, Massolini G, Temporini C, et al., editors. Analytical Quality by Design and Quality Control of drugs: from Quality Target Product Profile to the Analytical Target Profile. Book of Abstracts 29th International Symposium on Electro-and Liquid-Phase Separation Techniques-ITP 2023; 2023: 29th International Symposium on Electro-and Liquid-Phase Separation ....
- 33. Benetti C, Benetti AA. Quality by Design in Formulation Development. Introduction to Quality by Design (QbD) From Theory to Practice: Springer; 2024. p. 139-59.
- 34. Ames W. Critical quality attributes. Biosimilarity: The FDA Perspective. 2018:243.
- 35. Du R, Wang Y, Huang Y, Zhao Y, Zhang D, Du D, et al. Design and testing of hydrophobic core/hydrophilic shell nano/micro particles for drug-eluting stent coating. NPG Asia Materials. 2018;10(7):642-58.
- 36. Daneshmand S, Golmohammadzadeh S, Jaafari MR, Movaffagh J, Rezaee M, Sahebkar A, et al. Encapsulation challenges, the substantial issue in solid lipid nanoparticles characterization. Journal of cellular biochemistry. 2018;119(6):4251-64.
- 37. Hameed H, Rehman K, Hameed A, Qayuum A. Preparation and characterization of pH-responsive ionic crosslinked microparticles of mercaptopurine to target ulcerative colitis. Polymers and Polymer Composites. 2021;29(9 suppl):S1248-S56.
- 38. Mallah MA, Sherazi ST, Bhanger MI, Mahesar SA, Bajeer MA. A rapid Fourier-transform infrared (FTIR) spectroscopic method for direct quantification of paracetamol content in solid pharmaceutical formulations. Spectrochim Acta A Mol Biomol Spectrosc. 2015;141:64-70. https://doi.org/10.1016/j.saa.2015.01.036
- 39. Lengyel MB. FORMULATION STUDY OF MULTIPARTICULATES: MICROSPHERES AND MICROPELLETS 2022.
- 40. Leyva-Porras C, Cruz-Alcantar P, Espinosa-Solís V, Martínez-Guerra E, Piñón-Balderrama CI, Compean Martínez I, et al. Application of differential scanning calorimetry (DSC) and modulated differential scanning calorimetry (MDSC) in food and drug industries. Polymers. 2019;12(1):5.
- 41. Michelena LV, Bedogni GR, Jara MO, Williams III RO, Salomon CJ. Formulation and optimization of chitosan-based amorphous fenbendazole microparticles through a design of experiment approach. International Journal of Pharmaceutics. 2024;667:124872.
- 42. Almeida H, Ferreira B, Fernandes-Lopes C, Araújo F, Bonifácio MJ, Vasconcelos T, et al. Third-generation solid dispersion through lyophilization enhanced oral bioavailability of resveratrol. ACS Pharmacology & Translational Science. 2024;7(3):888-98
- 43. Sambuy Y, De Angelis I, Ranaldi G, Scarino M, Stammati A, Zucco F. The Caco-2 cell line as a model of the intestinal barrier: influence of cell and culture-related factors on Caco-2 cell functional characteristics. Cell biology and toxicology. 2005;21:1-26.
- 44. Riss TL, Moravec RA, Niles AL, Duellman S, Benink HA, Worzella TJ, et al. Cell viability assays. Assay guidance manual [Internet]. 2016.
- 45. Ma J, Yin G, Lu Z, Xie P, Zhou H, Liu J, et al. Casticin prevents DSS induced ulcerative colitis in mice through inhibitions of NF-κB pathway and ROS signaling. Phytotherapy Research. 2018;32(9):1770-83.
- 46. Goh FG, Banks H, Udalova IA. Detecting and Modulating the NF-kB Activity in Human Immune Cells: Generation of Human Cell Lines with Altered Levels of NF-κB. Inflammation and Cancer: Methods and Protocols: Volume 2: Molecular Analysis and Pathways. 2009:39-54.
- 47. Nam H, Lillehoj HS, Lee Y. Development of Antigen-Capture Enzyme-linked Immunoassay for Chicken Interleukin-34. Developmental & Comparative Immunology. 2025:105331.